Supplementary Figure 1: Gating strategy for sorting snMacs, onMacs and brain microglia for bulk RNA sequencing.

A: Representative gating strategy used to sort CD64+ snMacs (top) and purity check (down). The sciatic nerve from at least 5 mice were pooled and stained for the displayed surface markers. CD64+ cells among CD45+ cells were removed of doublets, dead cells, eosinophils, neutrophils and monocytes to obtain $CD11b^{Int\text{-}Hi}CD64^{Hi}$ snMacs.

B. Representative gating strategies used to sort CD64+F4/80+ snMacs macrophages (top), $CD45^{Lo}CD11b^{Hi}$ onMacs (middle) and $CD45^{Lo}CD11b^{Hi}$ brain microglia (bottom) are displayed. The sciatic nerves and optic nerves were harvested from the same mouse and nerves of five individual animals were pooled for one biological replicate. Four individual biological replicates from

independent experiments were submitted to RNA sequencing. For brain microglia, cells of five individual mice were sorted and submitted to RNA sequencing. Dump channel included antibodies against Ly6C, Ly6G, CD3e, CD19 and B220.

Supplementary Figure 2: Most genes identified by bulk transcriptomics are expressed by either epineurial and endoneurial snMacs.

A. Single-cell heatmap of the genes identified in Figure 1 by bulk transcriptomics plotted on the tSNE populations identified by sc-RNA-sequencing as Relmα^{+}Mgl1^{+} snMacs and Relmα^{-}Mgl1^{-} snMacs. **The heatmap shows the scaled log2 normalised expression values. The log2 normalised expression values were scaled using the 'scale_quantile' function of the SCORPIUS package with default parameters (v1.0).** **B.** tSNE plot depicting the expression of *Cx3cr1* in snMacs (left). Representative flow cytometry plots showing *Cx3cr1*^{gfp} expression in Mgl1^{-} snMacs (red) and Mgl1^{+} snMacs (blue). Data represents five pooled mice. **C.** Quantification of Cx3cr1-GFP^{+} Mgl1^{-} snMacs and Mgl1^{+} snMacs. Data are shown as mean ±SEM. Symbols represent individual animals. **D.** Representative confocal microscopy of sciatic nerve vibratome cross sections from Cx3cr1$^{gfp/wt}$ mice. Location of anti-GFP^{+}MGL1^{-} snMacs (filled arrowheads) and anti-GFP^{-}MGL1^{+} snMacs (open arrowheads) is depicted. Nuclei were counterstained with DAPI. Scale bar: overview 100µm, insets 20µm. Images are representative of three individual mice.

Supplementary Figure 3: Endoneurial snMacs express higher levels of immediate early response genes. A. Single-cell heatmap of the immediate early response genes induced by tissues digestions identified by Van Hove et al. and projected on the tSNE populations identified by sc-RNA-sequencing as Relmα^{+}Mgl1^{+} snMacs and Relmα^{-}Mgl1^{-} snMacs. **The heatmap shows the scaled log2 normalised expression values. The log2 normalised expression values were scaled using the 'scale_quantile' function of the SCORPIUS package with default parameters (v1.0).** **B.** tSNE plot depicting the expression of canonical immediate early response genes on Relmα^{+}Mgl1^{+} snMacs and Relmα^{-}Mgl1^{-} snMacs.

Supplementary Figure 4: Heterogeneity of CNS and PNS macrophages. A. tSNE plot containing the brain microglia and BAM populations described by Van Hove et al.[10], as well as our snMacs. CPhi-BAM: MHCII^{Hi} Macs from the choroid plexus. CPlo-BAM: MHCII^{Low} Macs from the choroid plexus. Dhi-BAM: MHCII^{Hi} Macs from the Dura mater. Dlo-BAM: MHCII^{Low} Macs from the Dura mater. SD-BAM: Macs from the Subdural meninges. Epineural snMacs: Relmα^{+}Mgl1^{+} snMacs. Endoneurial snMacs: Relmα^{-}Mgl1^{-} snMacs. B. Feature plots of various CNS and PNS Mac-associated genes.

Supplementary Figure 5: Mgl1+ epineurial macrophages express Lyve1 and are often located in close contact with blood vessels.
A. Expression of Lyve1 on snMacs subsets measured by flow cytometry. B. Representative histograms showing the expression of Lyve1 on Mgl1^{-} endoneurial snMacs (orange) and Mgl1^{+} epineurial snMacs (blue) over FMO controls (grey). (A, B) Data are representative of five individual animals. Cells from all individual mice were pooled after recording in one plot. C. Confocal microscopy was used to verify the location of Lyve^{+} cells within the epineurium of the sciatic nerve. Insets depict Lyve1^{+} cells in close proximity to CD31^{+}Collagen IV^{+} blood vessels (filled arrowheads). Not all Lyve1^{+} cells are found to be associated with the blood vessels (open arrowheads). D. F4/80^{+}Lyve^{-} endoneurial snMacs (open arrowheads) and F4/80^{+}Lyve1^{+} epineurial snMacs (filled arrowheads) are depicted. Note that single F4/80^{+} epineurial snMacs were found to be Lyve1^{-} (see R2). (C, D) The perineurium and the basal membranes of blood vessels were stained with Collagen IV. Nuclei were counterstained with DAPI. Images are representative of three individual mice.

Supplementary Figure 6: Monocyte recruitment upon sciatic nerve injury.
A. We defined a large gate, called the "Mono-Mac waterfall", containing Ly6C^{Hi} monocytes and CD64^{Hi} macrophages among CD45+CD11b+Ly6G-SiglecF- cells in the sciatic nerve. The cells within the Mono-Mac waterfall gate (green), were then divided based on their Ly6C and MHCII expression. At day 0.5, incoming monocytes (red) can still be distinguished from resident Macs (blue), even in

the MHCII^{Low} gate where the monocytes start to lose the Ly6C expression but still have lower CD64 expression. Once after Day 3, the Mono-Mac waterfall becomes one big continuum between Ly6C^{Hi} cells and CD64^{Hi} cells. B. Number of macrophages (as defined by the Mono-Mac waterfall in (A)), Ly6G+Ly6C+ neutrophils, SiglecF+ eosinophils, CD3+MHCII- T cells and CD19+MHCII+ B cells in the sciatic nerve at the indicated timepoints after the injury. Data shown as mean ±SEM from a representative experiment with 3 mice per time-point, except for day 37 (2 mice). Two independent kinetic experiments were performed in total.

Supplementary Figure 7: Relmα+ macrophage populations maintain their localization outside the nerve fascicles upon sciatic nerve injury and recovery. Confocal microscopy was performed on nerve cross sections isolated from mice at different time points (0, 0.5, 1.5, 5 and 14 days) after nerve crush. Upon injury, macrophages (marked by F4/80) accumulate both inside the nerve fascicles and in the surrounding connective tissues. MHCII^{Hi} and MHCII^{Low} macrophage subpopulations do not harbor a specific localization and seem randomly distributed in different regions of the nerve. In contrast, at all examined time points Relmα+ cells were exclusively present in perineurium and epineurium connective tissues outside the nerve fascicles. **Nerves from the different time points were collected from three separate nerve crush experiments (0.5 and 1.5 days; 0 and 5 days; 14 days) and images at each time point are representative of at least three individual mice.** Scale bar = 100μm.

Supplementary Figure 1

A Gating strategy Figure 1

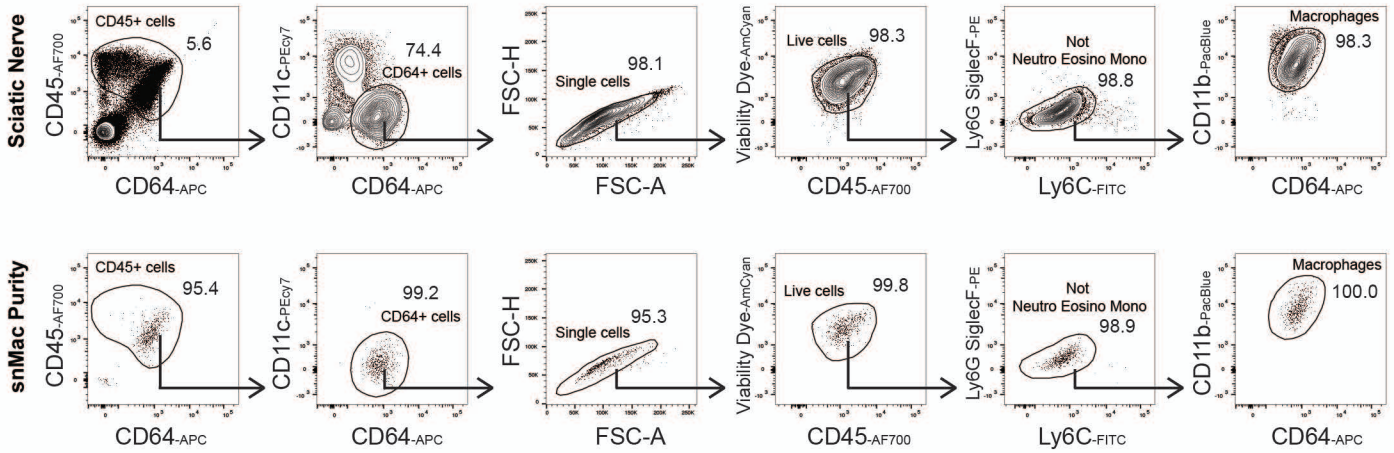

B Gating strategy Figure 2

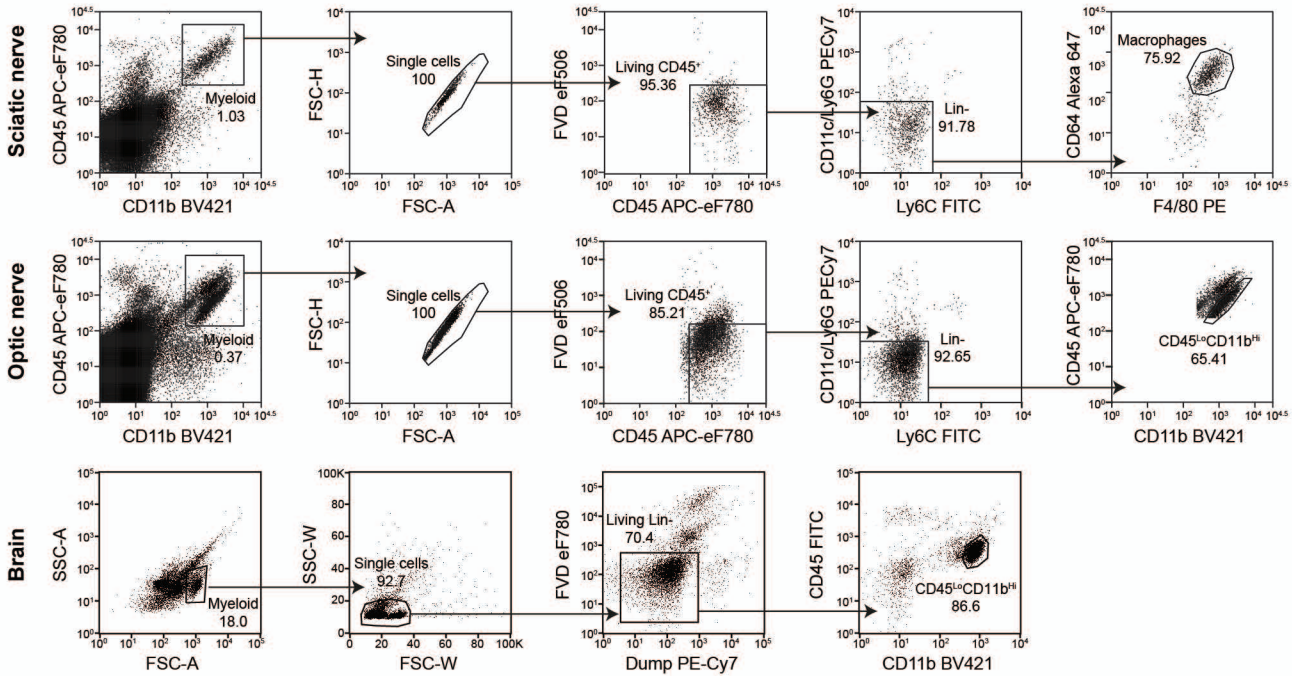

Supplementary Figure 2

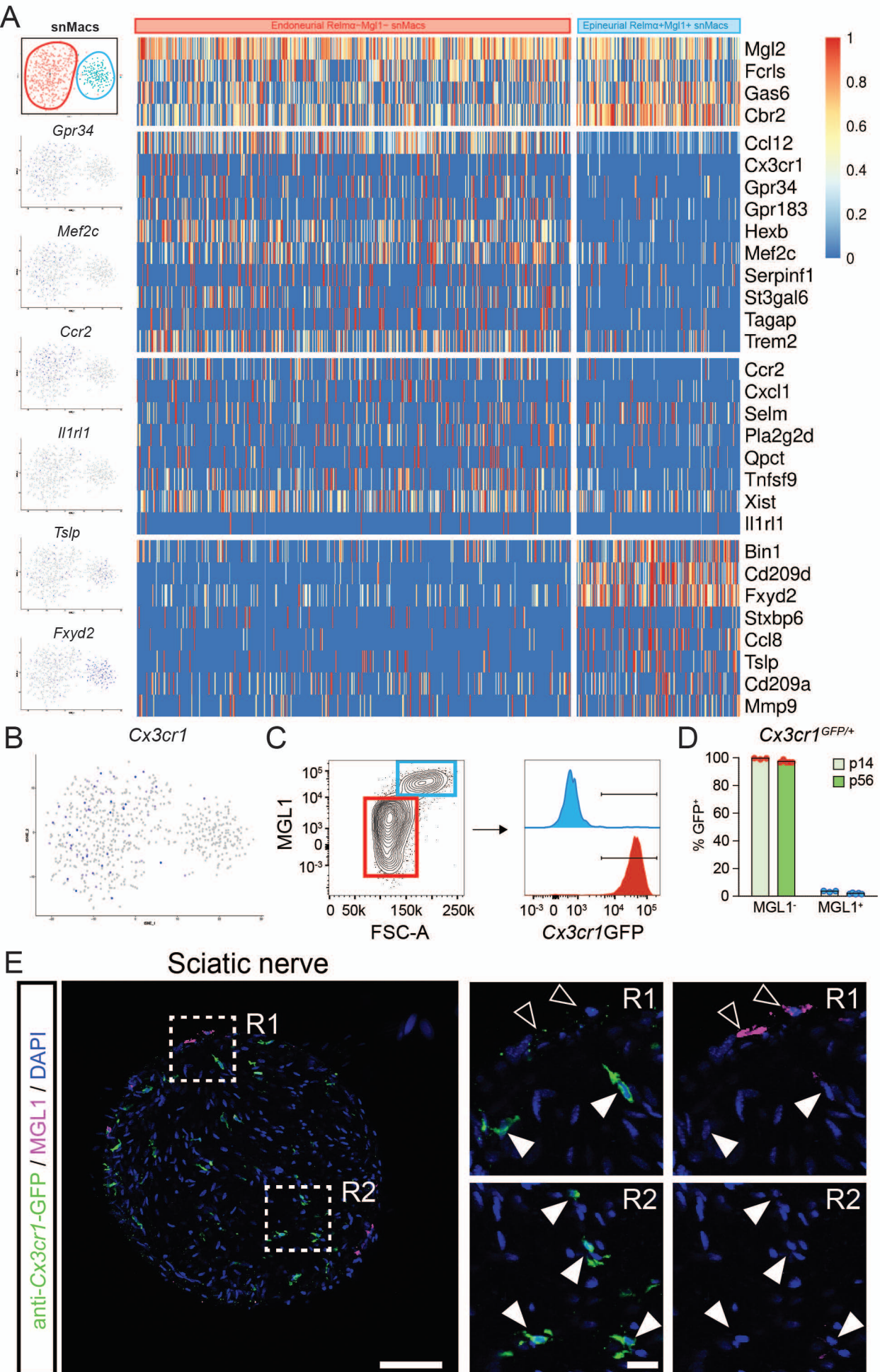

Supplementary Figure 3

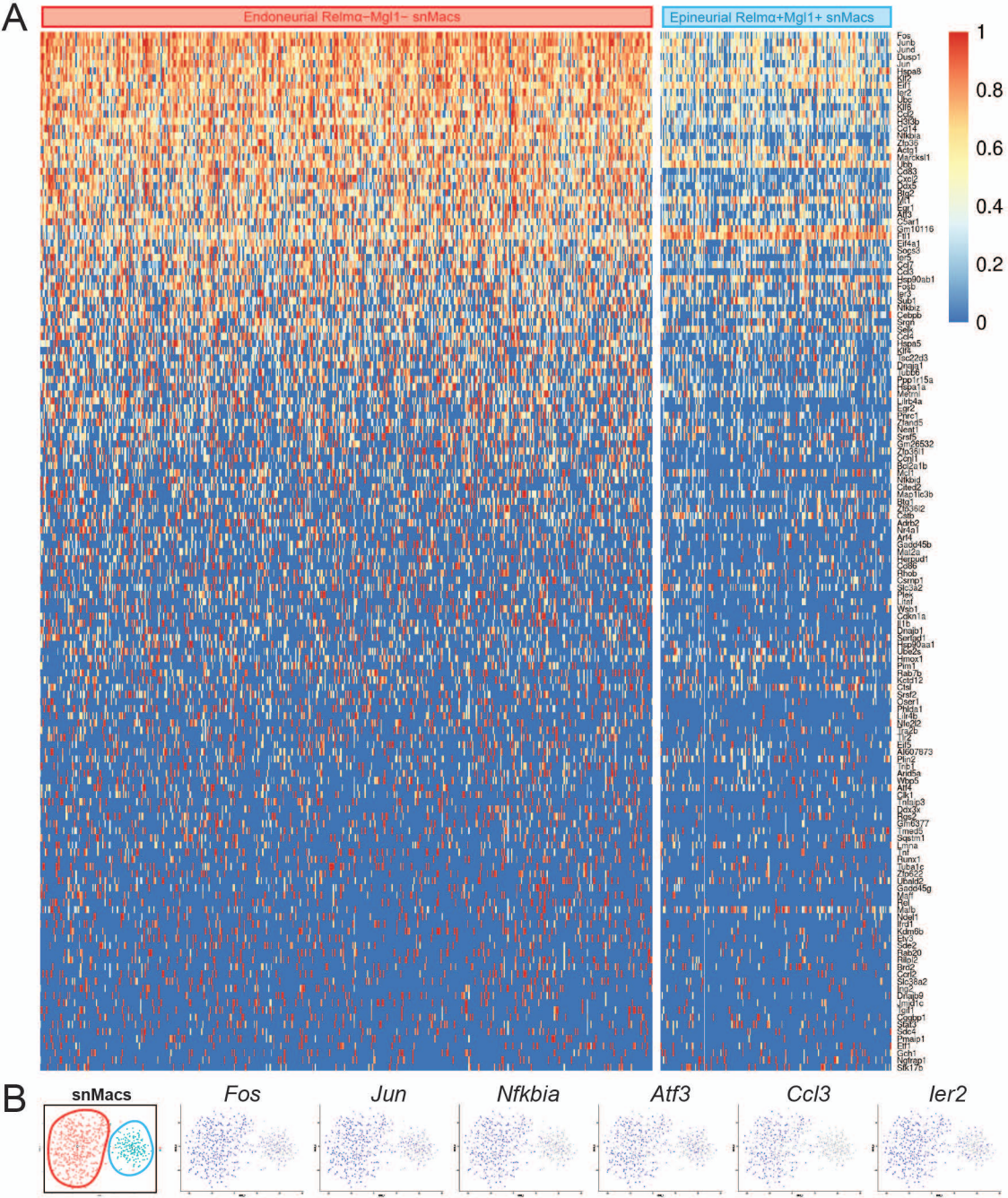

Supplemental Figure 4

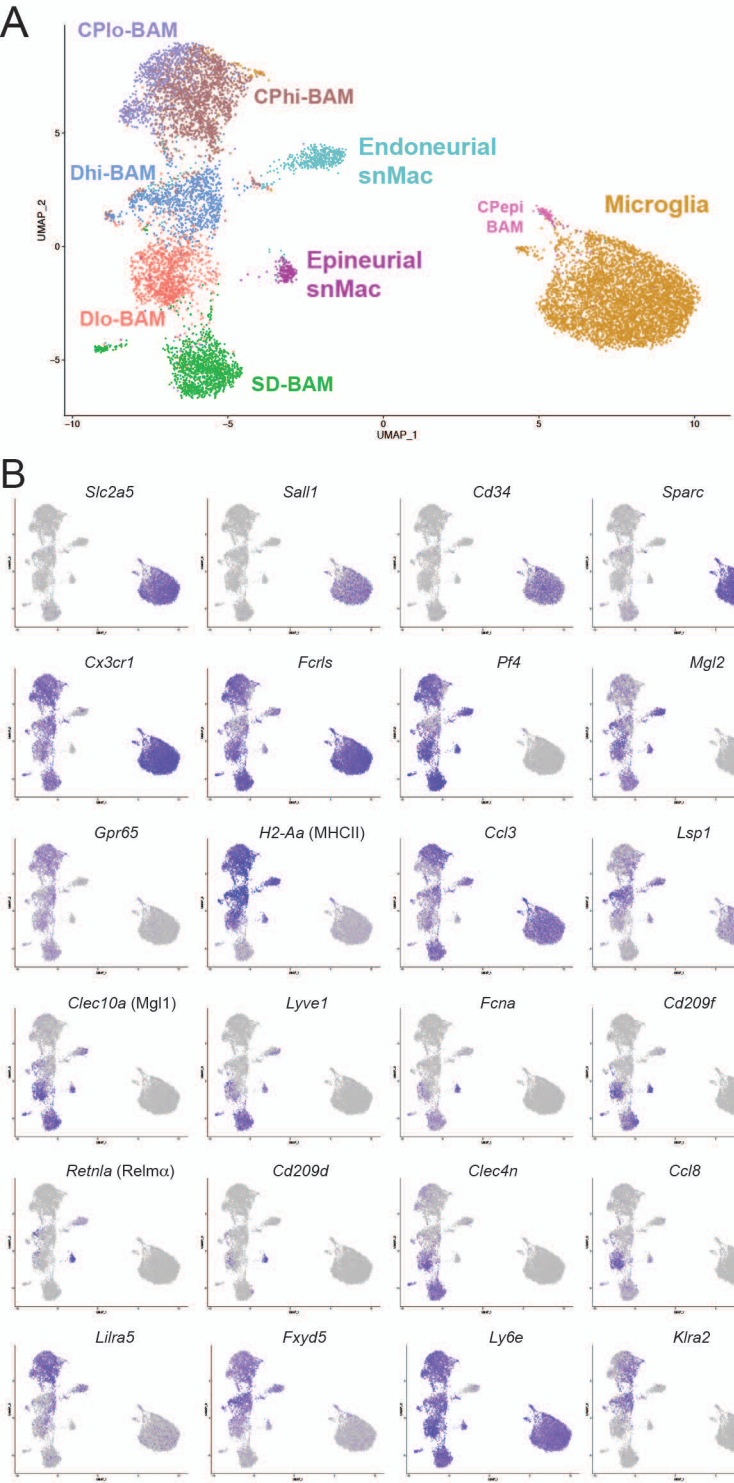

Supplementary Figure 5

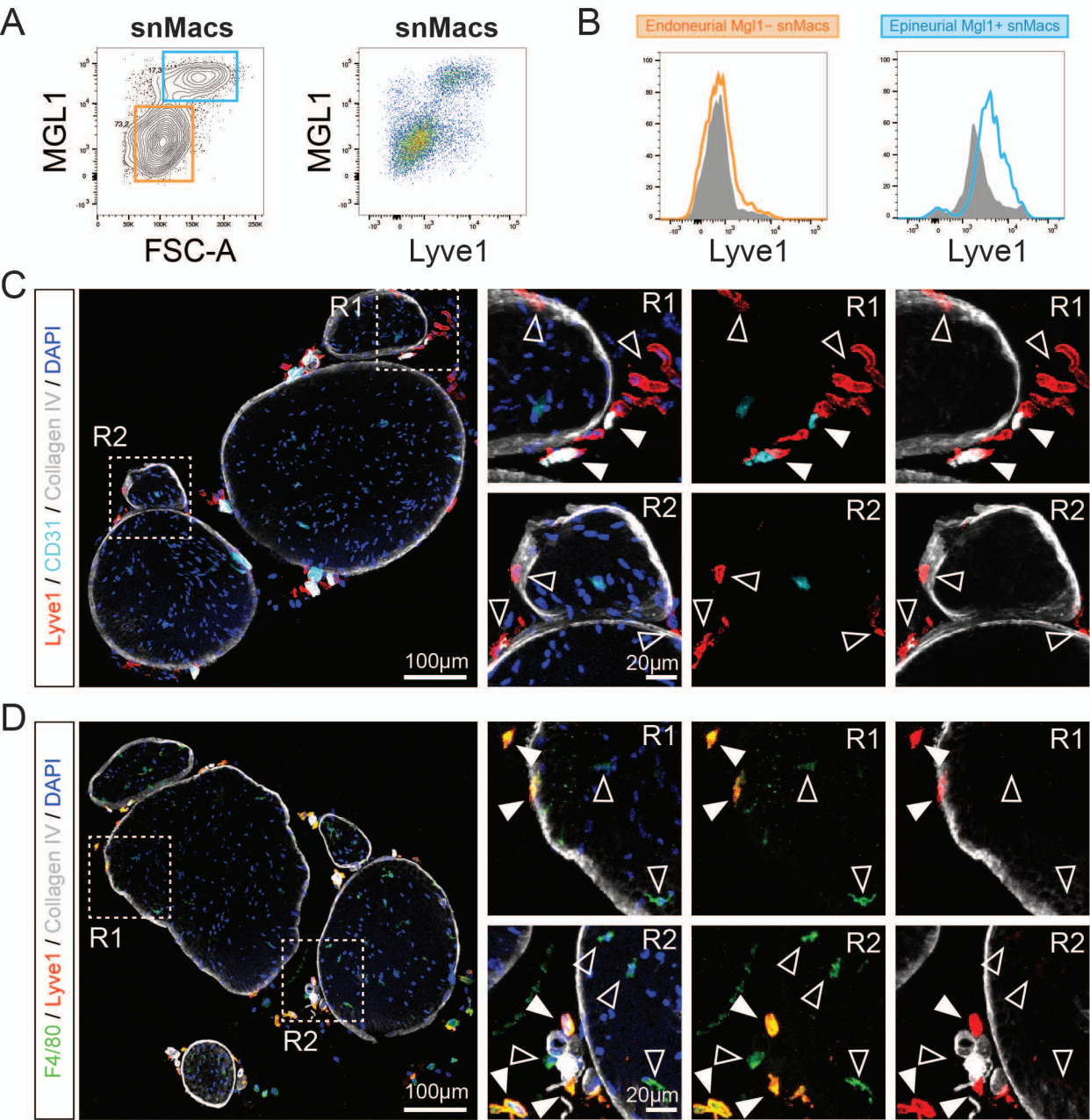

Supplementary Figure 6

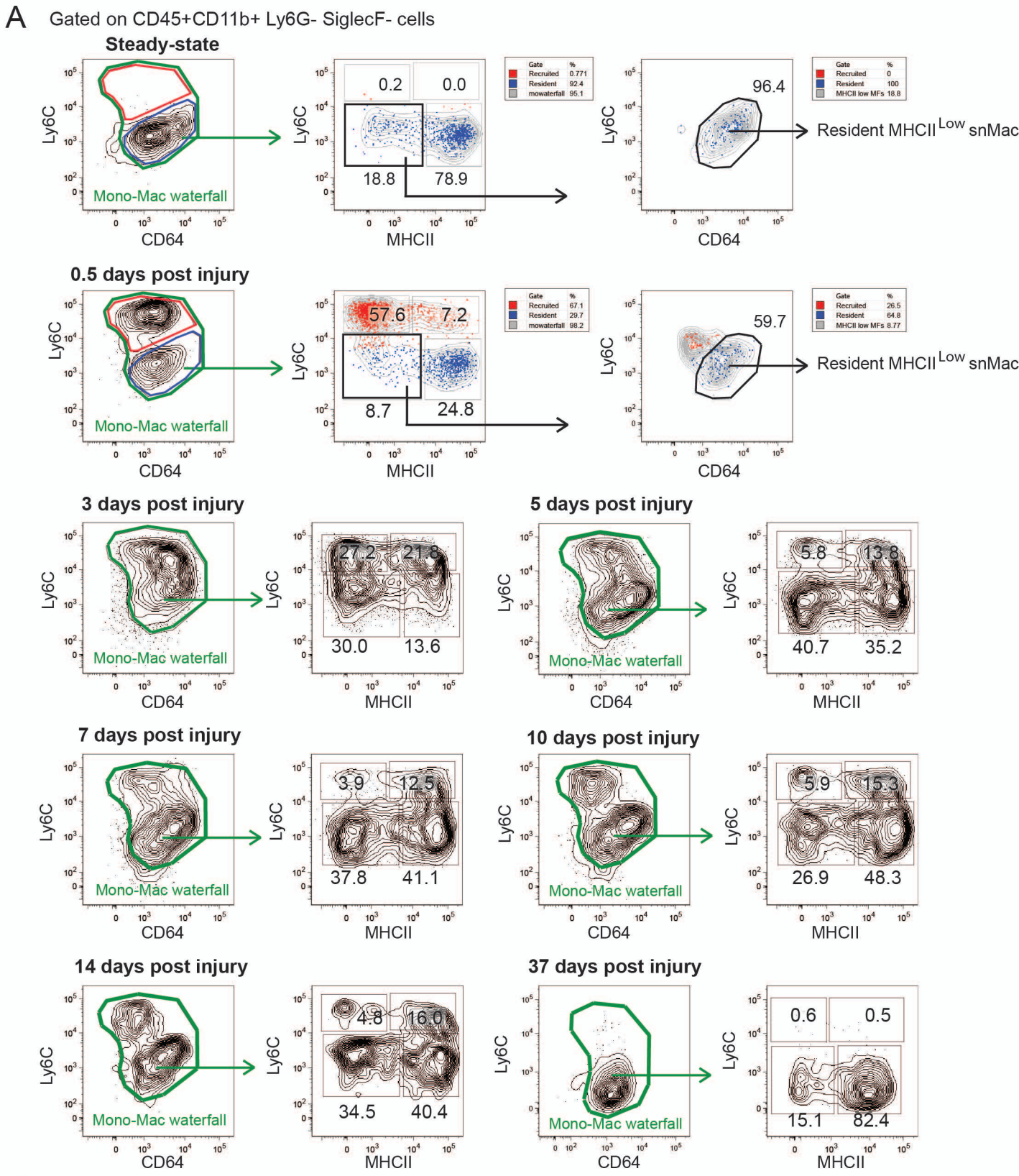

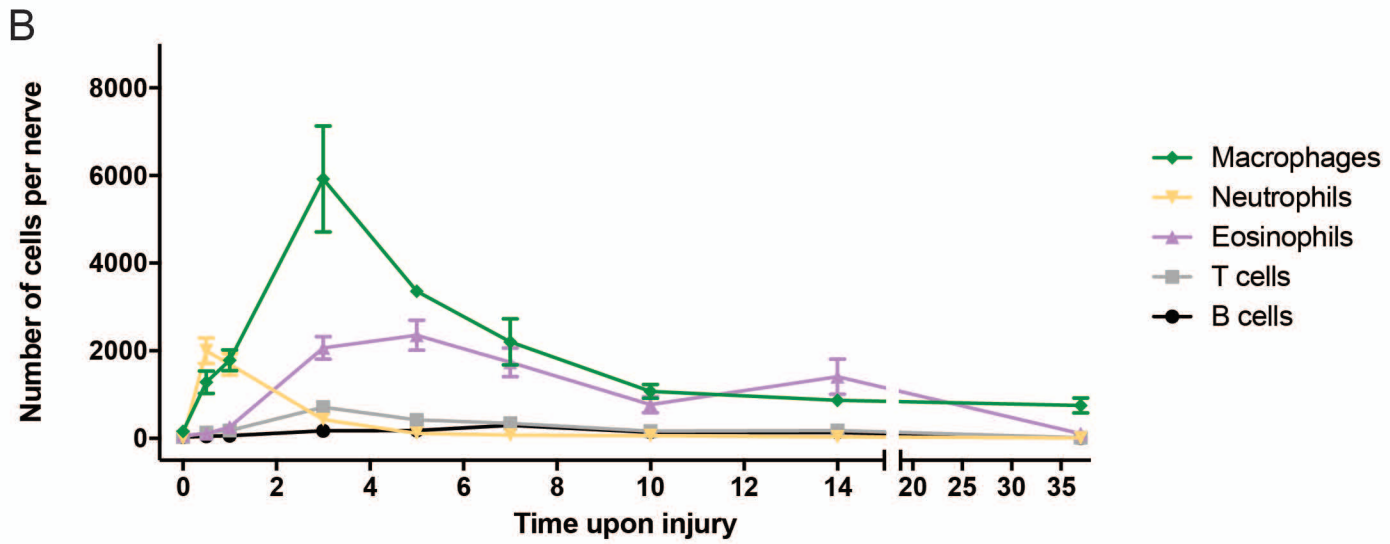

Supplementary Figure 7